

Stereodynamics and Characterization of the Hexa(4-*n*-dodecylbiphenyl)-benzene Hexaanion that Includes a Twisted Benzene Core

Lior Eshdat,^[a] Roy E. Hoffman,^[a] Andreas Fechtenkötter,^[b] Klaus Müllen,^[b] and Mordecai Rabinovitz*^[a]

Abstract: Hexa(4-*n*-dodecylbiphenyl)benzene (HDBB) was reduced by a series of alkali metals in THF under high vacuum. Three reduction states were identified by NMR spectroscopy, namely the dianion, tetraanion and hexaanion. The NMR spectra of HDBB⁶⁻ revealed a remarkable distortion of symmetry, which is interpreted by adoption of a twisted conformation of the central benzene ring and a slow rotation of the inner phenylene rings of the biphenyl units. Due to the surprising thermal stability of the hexaanion, a dynamic NMR investigation revealed the pseudorotation of the twisted conformation and the phenylene rotation mentioned above.

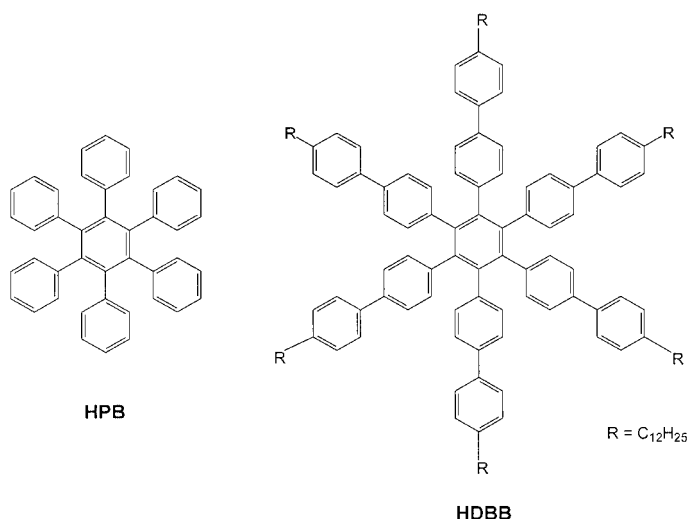
Keywords: alkali metals • carbanions • molecular dynamics • NMR spectroscopy • structure elucidation

Introduction

The addition of electrons to polycyclic aromatic hydrocarbons (PAHs)^[1] drastically modifies their physical and chemical characteristics including their structure and stereodynamic processes.^[2–4] Thus, in the phenyl-substituted benzenes *ortho*-terphenyl- and 1,2,4,5-tetraphenylbenzene the barrier for rotation of the phenyl rings about the formal single bonds was found to increase as a result of reduction.^[3, 4] The higher energy barrier suggests that more efficient conjugation increases the π bond order between the phenyl rings and the central benzene ring. For the same reason the torsional angles of the twisted systems are decreased upon charging.

We have recently investigated the reduction of hexaphenylbenzene (HPB) by alkali metals.^[4] Bart characterized the solid-state structure of neutral HPB by X-ray crystallography, showing that the central benzene ring is planar and the six attached phenyl groups form a propeller conformation ($\Phi \cong 67^\circ$) with a D_6 symmetry.^[5] The elongation of the C–C bonds between the central ring and the substituting phenyls to

merely a single bond (1.47–1.53 Å) is evidence for only partial conjugation. Phenyl rotation leads to enantiomerization of the right- and left-hand propellers, and this was studied by selective addition of substituents to the *ortho* and *meta* positions and by π complexation of only one of the phenyl rings. These studies afforded rotational barriers in the range of 12.2–33 kcal mol⁻¹.^[6] The unsubstituted HPB does not suffer from the additional steric interference and should therefore have even a lower rotational barrier.



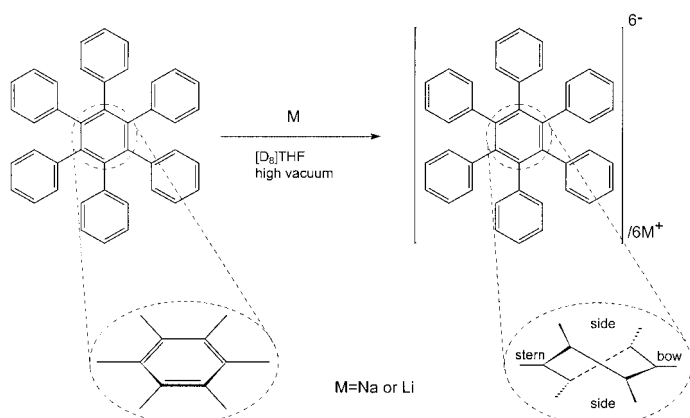
[a] Prof. M. Rabinovitz, L. Eshdat, Dr. R. E. Hoffman
Department of Organic Chemistry
The Hebrew University of Jerusalem, The Safra Campus
Givat-Ram, Jerusalem 91904 (Israel)
Fax: (+972)2-6527547
E-mail: mordecai@vms.huji.ac.il

[b] Dr. A. Fechtenkötter, Prof. Dr. K. Müllen
Max-Planck-Institut für Polymerforschung
Ackermannweg 10, 55128 Mainz (Germany)

Supporting information for this article (¹H and ¹³C NMR chemical shifts of the aromatic region of the Li, Na, K, and Rb salts of HDBB) is available on the WWW under <http://www.chemeurj.org> or from the author.

In our previous study we demonstrated that HPB is reduced to a hexaanion (HPB⁶⁻) characterized as six covalently linked benzyl anions, while the central benzene ring acts as an array of six benzyl functions. It has been shown that the central ring carries two charges, and adopts a nonaromatic twisted

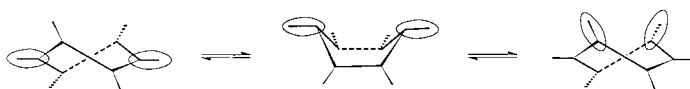
conformation (Scheme 1). There are only a handful of other examples of benzene rings that distort into twisted conformations, none of these were reduction products.^[7, 8]



Scheme 1. Reduction of HPB, indicating the “stern and bow” and “side” positions in the twisted conformation.

In a six-membered twisted ring there are two distinguishable positions of the ring: 1) “stern and bow” and 2) “side” positions in the ratio of 2:4 (Scheme 1). Hence, in HPB^{6-} there are two types of phenyl substituents in the ratio of 2:4. The phenyls attached to the “side” positions have a high phenyl rotation barrier, as evidenced by its ABCDE pattern in the NMR spectra.

Two dynamic processes can therefore take place:^[9] 1) a *pseudorotation* process of the six-membered twisted ring (Scheme 2), which interconverts two degenerate twisted conformations thus exchanging the “stern and bow” and the “side” sites of the phenyl substituents, and/or interconversion of two twisted enantiomers, which leads to enantiomerization;



Scheme 2. Pseudorotation of a twisted six-membered ring. Note the circled substituents that interchange positions.

Abstract in Hebrew:

תקציר

הקסא(4-*n*-דודצילביפניליל)בנזן (HDBB) חוזר על-ידי סדרה של מתכות אלקליות ב- $[\text{D}_8]\text{THF}$ תחת ואקום גבוה. שלוש דרגות חיזור זוהו בעזרת תמיג והם הדיאניון, הטטראאניון וההקסאניון. ספקטרום התמיג של HDBB^{6-} חשף עיוות סימטריה יוצא דופן, שפורש כאימוץ קונפורמציה סירה מעוותת על-ידי טבעת הבנזן המרכזית והאטה של סיבוב הפנילנים שבהיקף הפנימי. לאור היציבות התרמית המפתיעה של ההקסאניון, התאפשרה חקירת תמיג דינמי של הפסודורוטציה של קונפורמציות הטבעת המעוותת ושל סיבוב הפנילן שהוזכרו לעיל.

2) *phenyl rotation*, which exchanges the two different *ortho* sites as well as the *meta* positions of the asymmetrical “side” phenyl rings.

Due to thermal instability of HPB^{6-} , we could not follow these molecular dynamic processes on the NMR timescale. A second drawback of this instability was the incapability to perform a nucleophilic quench reaction that would chemically prove the hexaanionic state—our assignment had to be based exclusively on physical grounds.

We therefore extended our study to an analogous larger system, hexa(4-*n*-dodecylbiphenyl)benzene (HDBB),^[10] which could be described as a HPB in which each phenyl ring is substituted by another phenyl ring in the *para* position. The extended π system could stabilize the high levels of extra charge and, hence, would meet our objectives. HDBB itself forms ordered columnar mesophases with favorable properties.^[10b] It was prepared by a Kumada-type Grignard reaction of 4,4'-dibromotoluene with 4-*n*-dodecylphenylmagnesium bromide, catalyzed with $\text{PdCl}_2(1,1'$ -bis(diphenylphosphanyl)-ferrocene), to give di(4-*n*-dodecylbiphenyl)acetylene, which underwent a $\text{Co}(\text{CO})_8$ -catalyzed trimerization to HDBB in a 50% overall yield.^[10a]

In the present study we show that HDBB is reduced by alkali metals in THF to give the di-, tetra-, and hexaanions HDBB^{2-} , HDBB^{4-} , and HDBB^{6-} , respectively, thus producing another rare example of a PAH that reaches such high degrees of reduction.^[2i, 11] We demonstrate that the symmetry of HDBB^{6-} is distorted; this can be explained by the adoption of a twisted conformation of the central benzene ring and slowing of phenylene rotation. The surprising thermal stability of HDBB^{6-} allowed us to monitor the kinetic processes at elevated temperatures thus providing firm evidence for a complex stereodynamic situation.

Results and Discussion

Reduction of HDBB in $[\text{D}_8]\text{THF}$ was carried out by a potassium mirror under high vacuum in an extended NMR tube in a controlled fashion; this enabled us to spectroscopically monitor the formation of the different reduction states (Figure 1). After a few minutes of metal contact, the solution color changed to purple, and two broad sets of ^1H NMR chemical shifts appeared (Figure 1b). These two sets were assigned as species HDBB^{2-} and HDBB^{4-} , and each one of them maintained a spectral pattern similar to the starting material (two AB systems). The center of gravity of the aromatic signals of HDBB^{2-} and HDBB^{4-} was shifted upfield relative to that of the neutral species by 0.20 and 0.44 ppm, respectively. Further contact with the metal increased the intensities of the HDBB^{4-} signals at the expense of those of HDBB^{2-} until the latter disappeared (Figure 1c); the signals of HDBB^{4-} then became narrower, and a new NMR pattern (HDBB^{6-}) grew in parallel with a decrease in the signal intensities of HDBB^{4-} (Figure 1d). This new spectrum showed a center of gravity at even higher field than that of the previous two species (0.81 ppm upfield shift relative to the neutral center of gravity of the aromatic region). Finally, the spectrum exhibited exclusively HDBB^{6-} (Figure 1e). The

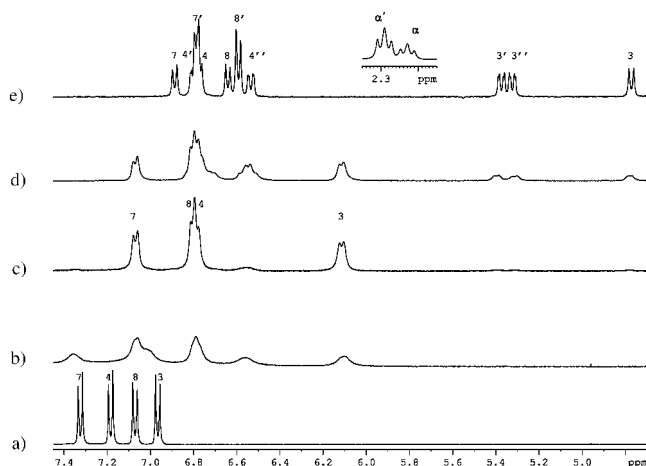


Figure 1. Aromatic region of the ^1H NMR spectra (400 MHz, $[\text{D}_8]\text{THF}$) of the diamagnetic products of reduction by potassium of HDBB. a) HDBB, RT; b) $\text{HDBB}^{2-} + \text{HDBB}^{4-}$, 210 K; c) HDBB^{4-} , 210 K; d) $\text{HDBB}^{4-} + \text{HDBB}^{6-}$, 210 K; e) HDBB^{6-} , RT, a breakdown in the symmetry of the molecule results in a set of ten doublets in the aromatic region and of two triplets (inset) in the benzyl region.

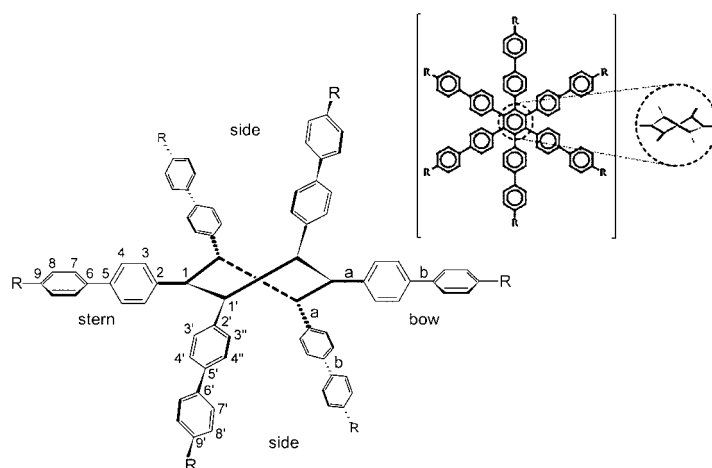
solution maintained a purple color throughout the whole reduction process.

The degree of reduction was determined 1) on the basis of the successive appearance of the species, 2) by a quenching reaction with D_2O , 3) by the redox reaction with the neutral compound, and 4) based on the upfield shift of the ^1H and ^{13}C NMR signals. After each stage of the reduction process, oxidation with oxygen regenerated the starting material; this indicated that none of the three species forms as a result of decomposition or protonation processes. The three species do not represent different conformations of the same reduction state, because the sequence of their appearance was not temperature dependent and only resulted from further contact between the organic solution and the metal. Further, conformational changes cannot explain the gradual shift to a higher field of the NMR signals. The total upfield shift of the ^{13}C NMR signals of an anion relative to the neutral compound ($\Sigma\Delta\delta$) is proportional to the number of electrons that were added to the π system, and in most PAHs $\Sigma\Delta\delta \approx 160$ ppm per extra electron.^[12] The $\Sigma\Delta\delta$ values for HDBB^{4-} and HDBB^{6-} were found to be 608 and 874 ppm, respectively, very close to the expected values. The $\Sigma\Delta\delta$ value for HDBB^{2-} was not available owing to the lack of a full assignment of its ^{13}C NMR signals. Hence, the assignment of HDBB^{2-} was based on being the first diamagnetic species, followed by the tetra- and hexaanions, and on a quenching reaction with D_2O that yielded dideutero-HDBB ($m/z = 2004.3 [M^+ + \text{H}]$).^[13] A similar reaction with HDBB^{4-} and D_2O yielded mainly tetradeutero-HDBB ($m/z = 2008.7 [M^+ + \text{H}]$). To establish the assignment of HDBB^{6-} and HDBB^{4-} , we performed a redox experiment, as described in Equation (1), in which two equivalents of HDBB^{6-} reacted with one equivalent of the neutral compound (under inert conditions).



Following our assumption concerning the reduction states, after addition of neutral HDBB, the 12 equivalents of charge should have been distributed over a total of three equivalents of HDBB, so the solution must have contained the suspected tetraanion. Indeed, after reaching equilibrium the solution contained three equivalents of the tetraanion, as observed by NMR spectroscopy. Further, a quenching reaction of HDBB^{4-} with D_2O yielded mainly tetradeutero-HDBB ($m/z = 2008.7 [M^+ + \text{H}]$).

The spectrum of HDBB^{6-} showed a duplication of lines, which is explained by the adoption of a conformation of a lower symmetry (D_2) such as that observed for hexaphenylbenzene, in which the central benzene ring exists in a twisted conformation as described in Scheme 3.^[14] Ten ^1H NMR



Scheme 3. Geometry of HDBB^{6-} . The central benzene ring is in a twisted conformation. The four “side”-attached biphenylene systems are in the same orientation relative to the main plane of the twisted central ring; the two “stern-and-bow”-attached biphenylene systems lie on the C_2 axis.

doublets and twenty ^{13}C NMR peaks appeared in the aromatic region, and included two types of benzyl signals as well as two central ring carbon signals. According to heteronuclear single-quantum correlation with improved sensitivity (HSQC/SI)^[15] and heteronuclear multiple-bond correlation (HMBC)^[16] experiments, four of the ^1H NMR doublets belong to one type of biphenylene system and six doublets belong to a second type. In the latter, the outer phenylene ring has two doublets of double intensity compared to the rest, and the other four belong to the inner phenylene ring. The two sets of biphenylene groups and benzyl positions are in line with a twisted six-membered ring as the central ring, which has two “stern and bow” carbons and four “side” carbons. However, this should result in two sets of four doublets (eight all together) in the ratio of 2:4 and only 18 aromatic ^{13}C NMR signals. The spectrum can be fully rationalized by a slow rotation about the inner biphenyl σ -bond and a fast rotation about the outer biphenyl σ -bond (Scheme 3). Thus, at slow rotation the inner phenylene rings should contribute four proton doublets as well as six carbon signals instead of two proton doublets and four carbon signals when a rapid rotation occurs, while the fast rotating outer phenylene rings should contribute the two doublets of double intensity and four

carbon signals. Owing to the C_2 axis that crosses the “stern and bow” biphenylene systems, these rings should contribute the same number of proton doublets (four) and carbon signals (eight) at any rate of the phenylene rotation. All the “side” substituents are in the same orientation relative to the main plane of the twisted structure of the central ring. Otherwise we would have witnessed an additional duplication of lines in the NMR spectra.

The hexaanion $HDBB^{6-}$ showed a surprisingly high thermal stability; we were able to record temperature-dependant 1H NMR spectra up to 415 K. When the sample was cooled to room temperature, the intact spectrum of $HDBB^{6-}$ did not indicate any decomposition.

The most dispersed signals of nuclei that exchange sites in the dynamic processes were the doublets of the protons *ortho* to the central benzene ring (Figure 2). At low temperatures, there were three such doublets, in accordance with the twisted

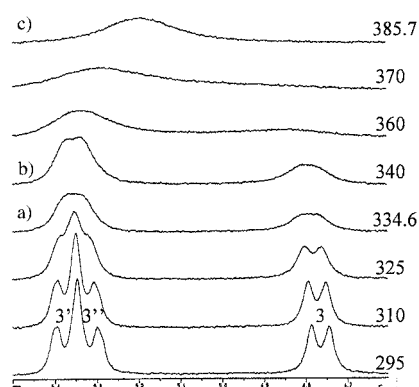


Figure 2. Temperature-dependent 1H NMR spectra (200 MHz, $[D_8]THF$) of positions 3, 3' and 3'' in $HDBB^{6-}$ (with potassium counterions). a) Coalescence of $H_{3'}$ and $H_{3''}$ attributed to phenylene rotation. b) The unified doublet of $H_{3'}$ and $H_{3''}$. c) Coalescence of H_3 and the unified doublet of $H_{3'}$ and $H_{3''}$ attributed to pseudorotation of the central benzene ring.

conformation, giving rise to two types of biphenylene groups, and with a slow phenylene rotation of the inner phenylenes about bond “a” (Scheme 3). They are designated as H_3 on the “stern/bow” biphenylene and H_3'/H_3'' on the “side” biphenylene. The H_3' proton is the one that is spatially closer to the “stern/bow” biphenylene than H_3'' , as determined from a larger NOE to protons H_3 and H_4 of the “stern/bow” biphenylene. Upon elevating the temperature the doublets of H_3'' and H_3' broadened and then coalesced at 335 K; this corresponds to a barrier of $\Delta G_{335}^\ddagger = 17.5 \pm 0.2 \text{ kcal mol}^{-1}$ for the phenylene rotation process that exchanges the magnetic sites of these two protons. At a temperature a few degrees higher their signals sharpened into a doublet. This new doublet broadened again and coalesced with the doublet of H_3 at 386 K as result of pseudorotation of the twisted benzene ring ($\Delta G_{386}^\ddagger = 18.3 \pm 0.3 \text{ kcal mol}^{-1}$). The barriers were calculated by using the Eyring equation and by assuming a transmission coefficient of unity.

Above 370 K the spectrum suffered from general line broadening, attributed to mixing of a low-lying triplet state into the electronic structure of the hexaanion that is more pronounced at higher temperatures. Therefore, EXSY (ex-

change spectroscopy) was implemented in order to follow the dynamics at lower temperatures.^[17] A cross-peak should appear in an EXSY experiment whenever a chemical exchange takes place between different spins during the mixing time (t_m) of a regular NOESY pulse sequence. The intensity of the cross-peak is dependent on the rate of exchange and on t_m . Measurements at different temperatures or with different t_m yield kinetic data of the exchange process, after taking into account statistical considerations. Thus, it allows us to detect processes in the timescale of t_m that are usually in the order of less than 1 Hz. It follows that this is superior to the conventional one-dimensional temperature-dependent 1H NMR spectroscopy. In one-dimensional experiments a broadening of the signals enables extraction of kinetic data only when the rate of the dynamic process approaches the frequency difference between the two exchanging signals, usually not less than a few dozens of Hz.

The results of the EXSY experiments are presented in Figure 3 and Table 1 and are fully in line with the kinetic data collected by regular temperature-dependent 1H NMR. In

Table 1. Kinetic data of the dynamic processes of $HDBB^{6-}$ (from EXSY).

	ΔH^\ddagger [kcal mol $^{-1}$]	ΔS^\ddagger [cal mol $^{-1}$]
pseudorotation ^[a]	16.3	− 5.4
phenylene rotation ^[b]	8.1	− 29.8

[a] Error estimation $\sim \pm 7\%$. [b] Error estimation $\sim \pm 2\%$.

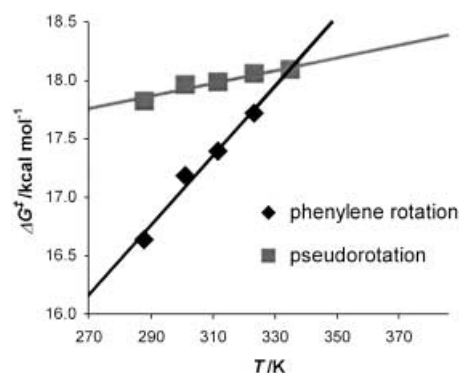


Figure 3. Free-energy barrier versus temperature as extracted from EXSY experiments of $HDBB^{6-}$.

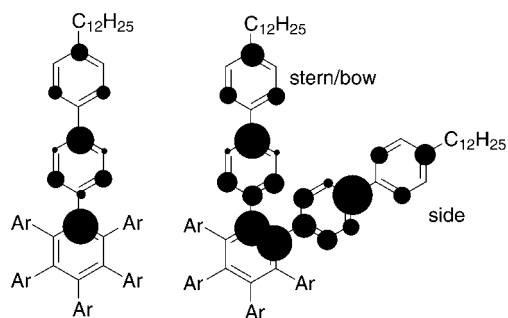
addition to the exchange between the H_3 , H_3' , and H_3'' positions, there is also an NOE contribution to the EXSY cross-peak, therefore the NOE effects were suppressed by a pulse sequence combined with rotational NOE. The processing of the data had to take into account statistical considerations due to the participation of the nuclei in both of the dynamic processes.

The dynamic behavior of $HDBB^{6-}$ could be explained by analyzing its electronic structure. A schematic picture of the charge distribution over the π system can be extracted from the differences between the ^{13}C NMR chemical shifts of an anion and its neutral parent compound.^[12] Equation (2)

$$Q_i = (\delta_{Ni} - \delta_{Ri})/K_C \quad (2)$$

describes the well-known correlation between the change in the chemical shift and the partial additional charge of a specific carbon in which Q_i is the partial charge, and δ_{Ni} and δ_{Ri} are the ^{13}C chemical shifts of carbon i in the neutral system and in a system in a reduction state R , respectively. K_C is derived by dividing $\Sigma\Delta\delta$ (see above) by R .

Table 2 shows the ^{13}C chemical shifts of HDBB, HDBB^{4-} , and HDBB^{6-} and the charge distribution of these anions. A schematic presentation of the charge distribution is shown in Scheme 4. In HDBB^{6-} the central benzene ring (C1 and C1'; Scheme 3) carries the highest amount of charge, which sums



Scheme 4. Schematic presentation of the charge distribution as calculated from ^{13}C NMR chemical shifts of HDBB^{4-} (left) and HDBB^{6-} (right). The dark circles represent partial charge.

up to 1.28 units of charge. This is a surprising result because one would expect the charge to spread out to the remote corners of the molecule due to charge repulsion.^[18] However, addition of electrons to a benzene ring contributes to its paratropic (antiaromatic) character, so it appears reasonable that only one ring “sacrifices” its aromaticity. The high charge density on the central benzene ring can rationalize the twisted conformation of the benzene ring, as a twisted conformation offers a more stable *nonaromatic* character. Additionally, the

twisted conformation creates a less encumbered environment for the phenylene rings, and thus a more efficient conjugation with the central ring.

The six phenylene rings of the inner rim carry much more charge than those of the outer rim (3.67 and 1.05 units of charge, respectively). Almost five out of the six charge units are delocalized over the central benzene ring and the first rim of phenylene rings that are attached to it, a moiety that resembles HPB.

The charge distribution shows a high resemblance to the charge distribution of biphenylmethylene anion.^[19] Except for the partial charge on C2 and C2', the charge is distributed in a charge alternation fashion (high charge density on the *ortho* and *para* positions)^[20] that is a general characteristic of phenyl substituents in carbanions^[3, 4, 21] and in particular of the biphenylmethylene anion. Like the biphenylmethylene anion, the rings close to the methylene position carry more charge than the remote phenylene rings. In this aspect, HDBB^{6-} may be viewed as a collection of six biphenylene methine anions that are connected through their methine positions to form a six-membered ring (the former central benzene ring). This is also the case for HPB^{6-} , which exhibits characteristics of six covalently linked benzyl anions.^[4]

As in HPB^{6-} , the delocalization of five charge units over the HPB moiety in HDBB^{6-} leads to higher conjugation between the phenylene rings and the central benzene ring, and, thus, to a higher barrier for phenylene rotation about the biphenyl bond marked “a” (Scheme 3). In contrast, the low charge density over the phenylene rings of the outer rim and their spatial environment is in line with the fact that there was no detectable slowing in their phenylene rotation rate about bond “b”. The similar steric effect and charge distribution over the two types of biphenylene systems makes it likely that the difference in the rotational barriers between bond “a” and “b” are similar for both “stern and bow” and “side” biphenylene systems. This cannot be spectroscopically ob-

Table 2. ^{13}C NMR chemical shifts of HDBB, HDBB^{4-} , and HDBB^{6-} (with potassium counterions) and the calculated partial charge.^[a]

Position number	HDBB		HDBB^{4-}		HDBB^{6-}		
	δ_i	δ_i	$\Delta\delta_i$	Q_i	δ_i	$\Delta\delta_i$	Q_i
1	141.42	109.28	-32.14	0.21	111.04	-30.38	0.21
1'	141.42	109.28	-32.14	0.21	108.72	-32.70	0.22
2	140.62	136.72	-3.90	0.03	128.56	-12.06	0.08
2'	140.62	136.72	-3.90	0.03	124.75	-15.87	0.11
3	132.97	123.61	-8.61	0.06	121.79	-11.18	0.08
3'	132.97	123.61	-8.61	0.06	116.22	-16.75	0.12
3''	132.97	123.61	-8.61	0.06	116.05	-16.92	0.12
4	125.67	124.36	-2.06	0.01	123.51	-2.16	0.01
4'	125.67	124.36	-2.06	0.01	117.90	-7.77	0.05
4''	125.67	124.36	-2.06	0.01	123.34	-2.33	0.02
5	138.53	115.24	-23.29	0.16	104.93	-33.60	0.23
5'	138.53	115.24	-23.29	0.16	102.06	-36.47	0.25
6	138.83	139.66	0.83	-0.01	139.19	0.36	0.00
6'	138.83	139.66	0.83	-0.01	139.60	0.77	-0.01
7	127.12	121.22	-5.90	0.04	118.29	-8.83	0.06
7'	127.12	121.22	-5.90	0.04	125.75	-1.37	0.01
8	129.33	128.98	-0.35	0.00	128.73	-0.60	0.00
8'	129.33	128.98	-0.35	0.00	128.85	-0.48	0.00
9	142.32	133.34	-8.98	0.06	127.67	-14.65	0.10
9'	142.32	133.34	-8.98	0.06	123.59	-18.73	0.13

[a] Q_i : calculated partial charge on carbon i ; δ_i : chemical shift of carbon i ; $\Delta\delta_i$: difference between the chemical shifts of the anion and the neutral carbon of carbon i .

served for the “stern and bow” biphenylene systems owing to the C_2 axis, which averages the two parts of the this system at any rate of rotation.

If $HDBB^{2-}$ and $HDBB^{4-}$ adopt a twisted conformation as well, then they would undergo a fast *pseudorotation*, since simplicity is maintained in both the 1H and ^{13}C NMR spectra even at 165 K. Otherwise, their central benzene ring would maintain its planarity or adopt a chair conformation that could still provide only one type of biphenylene substituents, if they all adopted the same axial/equatorial position.

We also chose to study the reduction of HDBB by lithium, sodium, and rubidium. All reduction processes were very similar to the reduction with potassium as described above, except for the following differences. When the reducing metal was lithium, the signals flattened before and after the appearance of the broad 1H NMR signals (7.6 Hz) of $HDBB^{2-}$. Only the aliphatic peaks were exhibited in ^{13}C NMR spectroscopy, and HSQCSI and HMBC experiments showed no cross-peaks, which are necessary for an assignment of the ^{13}C signals. With sodium, the reduction produced broad $HDBB^{2-}$ peaks (8.6 Hz) that did lead to a partial assignment of the ^{13}C NMR peaks of $HDBB^{2-}$, by the C–H correlation cross-peaks of the HSQCSI experiment. With either lithium or sodium the reduction progressed with the appearance $HDBB^{6-}$, showing only traces of $HDBB^{4-}$.

Only the chemical shifts of $HDBB^{6-}$ exhibit slight counterion dependence. In this highly charged reduction state, there should be a higher affinity of the cations towards the anion; hence the ion-pairing equilibrium^[22, 23] is shifted toward the contact ion pair. A closer interaction between the cations and the anion facilitates the acceptance of the extra electrons by reducing the Coulomb repulsion between the negative charges.^[24] The chemical shifts that showed the highest dependence belong to the carbon atoms of the central benzene with a standard deviation of 4.5 ppm compared to an average of 1.5 ppm of the outer carbons. These positions are potential locations for the counterion when the anion is in contact ion-pair status. The 7Li NMR spectra showed chemical shifts at -0.77 and -1.28 ppm (220 K, LiBr in $[D_8]THF$ as reference), which accompanied the 1H NMR spectra of $HDBB^{2-}$ and $HDBB^{6-}$, respectively. Lowering the temperature to 170 K caused a slight shift to a lower field of the former to -0.68 ppm, and a splitting into two signals of the latter (-0.63 and -2.04 ppm); this indicates that there are at least two different locations of the cations with respect to the anion that undergo through a fast exchange at higher temperatures. These chemical shifts are indicative of solvent-separated ion pairing (SSIP) as the dominant state in the ion-pairing equilibrium for the lithium salt.^[25] The $\Sigma\Delta\delta_C$ order of $Li > Na > K > Rb$ (919.5, 909.9, 873.6, and 854.5 ppm, respectively) points to a growing SSIP character with increasing size of the counter ion.

Conclusion

The reduction of the title compound with alkali metals constitutes a particularly striking example of an electron-transfer-induced structural change. In the case of the hexa-

anion it comprises the transition of an inner benzene ring from the conventional flat D_{6h} structure to a twisted arrangement. Thereby a complex stereodynamic situation arises, which, remarkably enough, could be fully analyzed by temperature-dependent NMR spectroscopy. Another favorable effect of the reduction process is the increased π bond order of formal single bonds in oligophenylene systems. This leads to higher activation barriers for rotation about the single bonds—processes that are often undetectable for the corresponding neutral compounds. Alkali metal derivatives are usually kinetically unstable and only exist in the absence of water. However, the mode of the extended π conjugation and the ion-pairing situation of the charged species of HDBB leads to a higher thermal stability, thus rendering extensive NMR studies feasible. Two features may finally be mentioned which place the above studies into even wider perspectives: 1) hexaphenylbenzene and hexa(biphenyl)benzene can undergo electron-transfer-induced cyclodehydrogenation processes under appropriate conditions affording extended polycyclic aromatic hydrocarbons,^[4, 10, 26, 27] and 2) such compounds have been shown to serve as core units for dendritic and hyperbranched polyphenylenes with penta- or hexaphenylbenzenes repeat units.^[28] Similar reduction experiments thus appear highly promising.

Experimental Section

The 1D and 2D NMR spectra were recorded on a Bruker DRX-400 pulsed FT spectrometer operating at 400.13, 100.62, and 155.51 MHz for 1H , ^{13}C , and 7Li NMR, respectively. Temperature-dependent 1H NMR spectra were recorded on a Bruker AMX-200 pulsed FT spectrometer operating at 200.06 MHz. Field-desorption (FD) mass spectroscopy measurements were taken on a VG Instrument ZAB2-SE-FPD. The synthesis of HDBB was reported previously.^[10a]

Preparation of the reduction samples: HDBB (5 mg) was added to a 5 mm NMR glass tube with an 8 mm extension. The alkali metal (kept in paraffin oil, cleaned from the oxidized layer and rinsed in petroleum ether 40–60 °C) was introduced under argon to the extension as a lithium wire or a piece of sodium/potassium/rubidium. The extended tube was then placed under high vacuum and dried by a flame. In the case of sodium, potassium, and rubidium, the metal was sublimed several times, creating a metal mirror on the 8 mm extension. Anhydrous $[D_8]THF$ (0.7 mL; dried over a sodium/potassium alloy under high vacuum) was vacuum transferred to the NMR tube and was degassed several times. Finally the extended tube was flame-sealed under high vacuum.

Controlled reduction process: The reduction took place when the $[D_8]THF$ solution was brought into contact with the metal by inversion of the sample and was stopped by returning the sample to the upright position, separating the metal from the solution.

Quenching reactions: Quenching with oxygen was performed under a nitrogen funnel. The sample was broken and the 8 mm extension containing the metal was removed. A mild stream of oxygen gas was bubbled through a syringe into the cooled solution until the color disappeared; this was followed by an examination by NMR spectroscopy. Reaction with D_2O was performed by breaking the sample in a glove box and pouring the solution into a vial containing D_2O (2 mL). The product was then extracted by dichloromethane and dried over magnesium sulfate; finally the solvent was evaporated. Field-desorption (FD) mass spectroscopy measurements of $[D_2]HDBB$ and $[D_4]HDBB$ ($m/z = 2004.3$ and 2008.7 [$M^+ + H$] (major peak), respectively) confirmed the degree of deuteration. MALDI-TOF spectra suffered from disproportionation and aromatization products that probably occur due to the laser excitation.

Oxidation of $HDBB^{6-}$ to $HDBB^{4-}$: A sample containing HDBB (4 mg, 2 μ mol) was reduced by a potassium mirror to $HDBB^{6-}$, as confirmed by

¹H NMR spectroscopy. The sample was broken in a glove box, and the glass chamber that contained the metal mirror was removed. Neutral HDBB (2 mg, 1 μmol) was added, and the NMR tube was capped. After 5 minutes at 220 K, the NMR spectrum showed broad lines of HDBB⁶⁻ and after 15 minutes the spectrum showed HDBB⁴⁻. An NMR spectrum of HDBB⁴⁻ after 24 h excludes possible oxidation by oxygen.

EXSY experiments: Samples for EXSY experiments were prepared by the same procedure as described above with the exception of dissolving the HDBB (1 mg, 0.5 μmol) in dry [D₈]THF (0.1 mL) in sealed 4 mm tubes with a minimum space above the solvent; this space contained the metal mirror. The 4 mm tubes were placed inside 5 mm NMR tubes. EXSY spectra were obtained with short mixing times relative to the longitudinal relaxation time (*t*₁). NOE effects were suppressed by combining with rotational NOE. Peak and multiplet volumes were measured by integration. Rate constants were determined from the integrals by using the matrix method described in the literature.^[29]

The peak intensity at zero time (*M*_{*i*}) is the sum of all the multiplets in that column corrected for relaxation effects. The intensity matrix (*I*) is then symmetrized for all *i* [Eq. (3)]:

$$M_{ij} = \exp(t_m/t_{1i}) \sum I_{ij} \quad (3)$$

The intensity matrix is symmetrized and normalized to yield *A* [Eq. (4)].

$$A_{ij} = (I_{ij} + I_{ji})/2\sqrt{(M_i M_j)} \quad (4)$$

The Jacobi transformation^[30] can then be used to find the natural logarithm of *A*. This is achieved by diagonalizing the matrix to yield its eigenvalues (*λ*), which are placed on the diagonal of an otherwise zero matrix, and eigenvectors (*X*), such that *f(A) = X⁻¹f(λ)X*. For a symmetric matrix *A*, its eigenvectors *X* are the transpose of their inverse so we have *f(A) = X^Tf(λ)X*. Dividing the natural logarithm of *A* by the mixing time yields the rate constant matrix *R* if the molar ratios (MR) are all one [Eq. (5)].

$$R_{ij} = -X^T(\ln \lambda)X/t_m \quad (5)$$

If the molar ratios are not all one then we get Equation (6):

$$R_{ij} = -X^T(\ln \lambda)X\sqrt{(MR_i/MR_j)}/t_m \quad (6)$$

NMR data: Chemical shifts (see Scheme 3) were measured relative to the downfield solvent peak, (temperature calibrated).^[31]

HDBB: ¹H NMR (400 MHz, [D₈]THF, RT): δ = 0.87 (t, ³J(H,H) = 6.80 Hz, 18H; H_μ), 1.27 (br, 108H; H_γ–H_λ), 1.56 (tt, ³J(H,H) = 7.38, 6.48 Hz, 12H; H_β), 2.53 (t, ³J(H,H) = 7.38 Hz, 12H; H_α), 6.96 (d, ³J(H,H) = 8.01 Hz, 12H; H₃), 7.07 (d, ³J(H,H) = 8.19 Hz, 12H; H₈), 7.18 (d, ³J(H,H) = 8.01 Hz, 12H; H₄), 7.32 ppm (d, ³J(H,H) = 8.19 Hz, 12H; H₇); ¹³C NMR (100 MHz, [D₈]THF, RT): δ = 14.43, 23.55, 30.19, 30.30, 30.47, 30.56, 30.58, 30.61, 30.64, 32.43, 32.87, 36.29 ppm (Ca); aromatic signals are presented in Table 2; ¹H and ¹³C NMR data in C₂D₂Cl₄ are reported in reference [10a].

K₂⁺[HDBB]²⁻: ¹H NMR (400 MHz, [D₈]THF, 220 K): δ = 1.50, 2.49, 6.50, 6.95, 7.33 ppm (all broad).

K₄⁺[HDBB]⁴⁻: ¹H NMR (400 MHz, [D₈]THF, 210 K): δ = 0.88 (t, ³J(H,H) = 6.60 Hz, 18H; H_μ), 1.26 (br, 108H; H_γ–H_λ), 1.49 (br, 12H; H_β), 2.40 (br, 12H; H_α), 6.10 (d, ³J(H,H) = 7.34 Hz, 12H; H₃), 6.78 (d, ³J(H,H) = 7.34 Hz, 12H; H₄), 6.80 (d, ³J(H,H) = 7.34 Hz, 12H; H₇), 7.07 ppm (d, ³J(H,H) = 7.34 Hz, 12H; H₈); ¹³C NMR (100 MHz, [D₈]THF, 210 K): δ = 14.82 (C_μ), 23.92, 30.53, 30.82, 31.02, 31.07, 33.20, 33.44 (C_β), 36.46 ppm (C_α); aromatic signals are presented in Table 2.

K₆⁺[HDBB]⁶⁻: ¹H NMR (400 MHz, [D₈]THF, RT): δ = 0.88 (t, ³J(H,H) = 6.60 Hz, 4H; H_μ), 0.89 (t, ³J(H,H) = 6.60 Hz, 8H; H_{μ'}), 1.27–1.32 (br, 108H; H_γ–λ) 1.40–1.54 (m, 12H; H_β) 2.31 (t, ³J(H,H) = 7.52 Hz, 4H; H_α), 2.37 (t, ³J(H,H) = 7.16 Hz, 8H; H_{α'}), 4.77 (d, ³J(H,H) = 8.62 Hz, 4H; H₃), 5.32 (dd, ³J(H,H) = 9.35, ⁴J(H,H) = 2.20 Hz, 4H; H_{3''}), 5.37 (dd, ³J(H,H) = 9.35, ⁴J(H,H) = 2.20 Hz, 4H; H_{3'}), 6.53 (dd, ³J(H,H) = 9.35, ⁴J(H,H) = 2.20 Hz, 4H; H_{4''}), 6.59 (d, ³J(H,H) = 8.44 Hz, 8H; H_{8'}), 6.64 (d, ³J(H,H) = 8.07 Hz, 4H; H₈), 6.77 (d, ³J(H,H) = 8.62 Hz, 4H; H₄), 6.79 (d, ³J(H,H) = 8.44 Hz, 8H; H_{7'}), 6.80 (dd, ³J(H,H) = 9.17, ⁴J(H,H) = 2.20 Hz, 4H; H_{4'}), 6.89 ppm (d, ³J(H,H) = 8.07 Hz, 4H; H₇); ¹³C NMR (100 MHz,

[D₈]THF, RT): δ = 14.50 (C_μ), 23.62, 30.38, 30.66, 30.70, 30.75, 30.81, 33.04 (C_β), 33.10 (C_β'), 36.36 (C_{α'}), 36.48 ppm (C_α); aromatic signals are presented in Table 2.

Acknowledgement

We are indebted to Professor Silvio Biali for very fruitful discussions. We would also wish to thank Dr. Hans Joachim Räder for mass spectroscopy measurements. This research was supported by The Israel Science Foundation (grant no. 147/00), by the Eshkol Foundation (The Ministry of Science, Israel), and by the Bundesministerium für Bildung und Forschung (Zentrum für multifunktionelle Werkstoffe und miniaturisierte Funktionseinheiten).

- [1] a) R. G. Harvey, *Polycyclic Aromatic Hydrocarbons*, Wiley-VCH, New York, **1997**; b) H. Hopf, *Classics in Hydrocarbon Chemistry: Syntheses, Concepts, Perspectives*, Wiley-VCH, Weinheim, New York, **2000**.
- [2] Selected examples: a) T. J. Katz, *J. Am. Chem. Soc.* **1960**, *82*, 3784–3785; 3785–3786; b) L. A. Paquette, *Pure Appl. Chem.* **1982**, *54*, 987–1004, and references therein; c) K. Müllen, J. F. M. Oth, H.-W. Engels, E. Vogel, *Angew. Chem.* **1979**, *91*, 251–253; *Angew. Chem. Int. Ed. Engl.* **1979**, *18*, 229–231; d) Y. Cohen, J. Klein, M. Rabinovitz, *J. Chem. Soc. Chem. Commun.* **1986**, 1071–1073; e) W. Heinz, H.-J. Räder, K. Müllen, *Tetrahedron Lett.* **1989**, *30*, 159–162; f) A. Sekiguchi, K. Ebata, C. Kabuto, H. Sakurai, *J. Am. Chem. Soc.* **1991**, *113*, 1464–1465; g) H. Bock, K. Gharagozloo-Hubmann, C. Näther, N. Nagel, Z. Havlas, *Angew. Chem.* **1996**, *108*, 720–721; *Angew. Chem. Int. Ed. Engl.* **1996**, *35*, 631–632; h) P. Boman, B. Eliasson, R. A. Grimm, G. S. Martin, J. T. Strnad, S. W. Staley, *J. Am. Chem. Soc.* **1999**, *121*, 1558–1564; i) M. Rabinovitz, R. Benshafut, E. Shabtai, L. T. Scott, *Eur. J. Org. Chem.* **2000**, 1091–1106 and references therein.
- [3] a) W. Huber, A. May, K. Müllen, *Chem. Ber.* **1981**, *114*, 1318–1336; b) W. Huber, K. Müllen, *Acc. Chem. Res.* **1986**, *19*, 300–306.
- [4] L. Eshdat, A. Ayalon, R. Beust, R. Shenhar, M. Rabinovitz, *J. Am. Chem. Soc.* **2000**, *122*, 12637–12645.
- [5] J. C. J. Bart, *Acta Crystallogr. Sect. B.* **1968**, *24*, 1277–1287.
- [6] a) D. Gust, A. Patton, *J. Am. Chem. Soc.* **1978**, *100*, 8175–8181; b) B. Mailvaganan, B. G. Sayer, M. J. McGlinchey, *J. Organomet. Chem.* **1990**, *395*, 177–185.
- [7] Tris(donor)–tris(acceptor)-substituted benzenes: a) J. J. Wolff, S. F. Nelsen, D. R. Powell, *J. Org. Chem.* **1991**, *56*, 5908–5911; b) J. J. Wolff, H. Irngartinger, F. Gredel, I. Bolocan, *Chem. Ber.* **1993**, *126*, 2127–2131.
- [8] Dications of alkylated hexaaminobenzene: J. M. Chance, B. Kahr, A. B. Buda, J. P. Toscano, K. Mislow, *J. Org. Chem.* **1988**, *53*, 3226–3232.
- [9] J. Sandström, *Dynamic NMR Spectroscopy*, Academic Press, London, **1982**.
- [10] a) A. Fechtenkötter, K. Saalwächter, M. A. Harbison, K. Müllen, H. W. Spiess, *Angew. Chem.* **1999**, *111*, 3224–3228; *Angew. Chem. Int. Ed.* **1999**, *38*, 3039–3042; b) Y. Geng, A. Fechtenkötter, K. Müllen, *J. Mater. Chem.* **2001**, *11*, 1634–1641.
- [11] a) J. Heinze, *Angew. Chem.* **1981**, *93*, 186–187; *Angew. Chem. Int. Ed. Engl.* **1981**, *20*, 202–203; b) J. Heinze, *Angew. Chem.* **1984**, *96*, 823–839; *Angew. Chem. Int. Ed. Engl.* **1984**, *23*, 831–847; c) A. de Meijere, J. Heinze, K. Meerholz, O. Reiser, B. König, *Angew. Chem.* **1990**, *102*, 1443–1444; *Angew. Chem. Int. Ed. Engl.* **1990**, *29*, 1418–1419; d) J. Mortensen, J. Heinze, H. Herbst, K. Müllen, *J. Electroanal. Chem.* **1992**, *324*, 201–217; e) O. Reiser, B. König, K. Meerholz, J. Heinze, T. Wellauer, F. Gerson, R. Frim, M. Rabinovitz, A. de Meijere, *J. Am. Chem. Soc.* **1993**, *115*, 3511–3518; f) U. Müller, M. Baumgarten, *J. Am. Chem. Soc.* **1995**, *117*, 5840–5850.
- [12] a) G. Fraenkel, R. E. Carter, A. McLachlan, J. H. Richards, *J. Am. Chem. Soc.* **1960**, *82*, 5846–5850; b) H. Spiess, W. G. Schneider, *Tetrahedron Lett.* **1961**, 468–472; c) D. G. Farnum, *Adv. Phys. Org. Chem.* **1975**, *11*, 123–175; d) B. Eliasson, U. Edlund, K. Müllen, *J.*

- Chem. Soc. Perkin Trans. 2* **1986**, 937–940; e) K. Müllen, *Chem. Rev.* **1984**, *84*, 603–646.
- [13] Lithium reduction afforded a clean NMR spectrum of HDBB²⁻.
- [14] A boat structure can also explain the NMR spectra, but relying on the DFT calculations of HPB,^[4] which state that the twisted conformation is a minimum, while the boat is a transition state, and on the assumption that the HPB fragment in HDBB dictates the conformation, we chose the twisted conformation for further discussion.
- [15] L. E. Kay, P. Keifer, T. Saarinen, *J. Am. Chem. Soc.* **1992**, *114*, 10663–10635.
- [16] T. D. W. Claridge *Tetrahedron Organic Chemistry Series, Vol 19: High-Resolution NMR Techniques in Organic Chemistry* (Eds.: J. E. Baldwin, F. R. S and R. M. Williams), Oxford, Pergamon, **1999**, pp. 244–251
- [17] a) G. E. Hawkes, L. Y. Lian, E. W. Randall, K. D. Sales, *J. Magn. Reson.* **1985**, *65*, 173–177; b) C. L. Perrin, T. J. Dwyer, *Chem. Rev.* **1990**, *90*, 935–967; c) K. G. Orrell, V. Šik, *Annu. Rep. NMR Spectrosc.* **1993**, *27*, 163–171.
- [18] M. Baumgarten, U. Anton, L. Gherghel, K. Müllen, *Synth. Met.* **1993**, *57*, 4807–4812.
- [19] S. E. Browne, S. E. Asher, E. H. Cornwall, J. K. Frisoli, L. J. Harris, E. A. Salot, E. A. Sauter, M. A. Trecocke, P. S. Veale, Jr., *J. Am. Chem. Soc.* **1984**, *106*, 1432–1440.
- [20] a) J. Klein, *Tetrahedron* **1983**, *39*, 2733–2759; b) Y. Cohen, J. Klein, M. Rabinovitz, *J. Am. Chem. Soc.* **1988**, *110*, 4634–4640.
- [21] Selected examples: a) A. Carrington, J. dos Santos-Veiga, *Mol. Phys.* **1962**, *5*, 21–29; b) K. H. Hausser, L. Mongini, R. von Z. Steenwinkel, *Z. Naturforsch. Teil A* **1963**, *19*, 777–780; c) R. Biehl, K.-P. Dinse, K. Möbius, *Chem. Phys. Lett.* **1971**, *10*, 605–609; d) M. Plato, R. Biehl, K. Möbius, K. P. Dinse, *Z. Naturforsch. A* **1976**, *31*, 169–176; e) R. E. Jesse, P. Biloen, R. Prins, J. D. W. van Voorst, G. J. Hoijsink, *Mol. Phys.* **1963**, *6*, 633–635; f) A. Fürstner, G. Seidel, H.-E. Mons, R. Mynott, *Eur. J. Inorg. Chem.* **1998**, 1771–1774; g) B. Böhlér, D. Hüls, H. Günther, *Tetrahedron Lett.* **1996**, *37*, 8719–8722; h) M. Christl, H. Müller, *Chem. Ber.* **1993**, *126*, 529–535; i) H. Fujiwara, A. Yoshino, Y. Yokoyama, K. Takahashi, *Bull. Chem. Soc. Jpn.* **1992**, *65*, 2162–2167.
- [22] The term “ion pair” does not necessarily reflect reality in highly reduced species as more than one cation may be in contact with the anion.
- [23] a) M. Szwarc in *Ions and Ion Pairs in Organic Chemistry, Vol. 1.* (Ed.: M. Szwarc), Wiley, New York, **1972**; b) M. Szwarc, *Pure Appl. Chem.* **1976**, *48*, 247–250.
- [24] M. Baumgarten, K. Müllen, *Top. Curr. Chem.* **1994**, *169*, 1–103, and references therein.
- [25] A. Ayalon, Ph.D. Thesis, The Hebrew University of Jerusalem (Israel), **1994**.
- [26] a) A. M. van de Craats, J. M. Warman, A. Fechtenkötter, J. D. Brand, M. A. Harbison, K. Müllen *Adv. Mater.* **1999**, *11*, 1469–1472; b) I. Fischbach, T. Pakula, P. Minkin, A. Fechtenkötter, K. Müllen, H. W. Spiess, K. Saalwächter *J. Phys. Chem. B* **2002**, *106*, 6408–6418; c) M. Lee, J.-W. Kim, S. Peleshanko, K. Larson, Y.-S. Yoo, D. Vaknin, S. Markutsya, V. V. Tsukruk, *J. Am. Chem. Soc.* **2002**, *124*, 9121–9128. d) C. D. Simpson, J. D. Brand, A. J. Berresheim, L. Przybilla, H. J. Räder, K. Müllen *Chem. Eur. J.* **2002**, *8*, 1424–1429.
- [27] H. Bock, Z. Havlas, K. Gharagozloo-Hubmann, M. Sievert, *Angew. Chem.* **1999**, *111*, 2379–2382; *Angew. Chem. Int. Ed.* **1999**, *38*, 2240–2243.
- [28] a) F. Morgenroth, E. Reuther, K. Müllen, *Angew. Chem.* **1997**, *109*, 647–649; *Angew. Chem. Int. Ed. Engl.* **1997**, *36*, 631–634; b) F. Morgenroth, K. Müllen *Tetrahedron* **1997**, *53*, 15349–15366; c) M. Müller, C. Kübel, K. Müllen *Chem. Eur. J.* **1998**, *4*, 2099–2109; d) U.-M. Martin, K. Müllen, *Chem. Commun.* **1999**, 2293–2294; e) U.-M. Wiesler, A. J. Berresheim, F. Morgenroth, G. Lieser, K. Müllen, *Macromolecules* **2001**, *34*, 187–199; f) R. E. Bauer, V. Enkelmann, U.-M. Wiesler, A. J. Berresheim, K. Müllen, *Chem. Eur. J.* **2002**, *8*, 3858–3864.
- [29] B. A. Johnson, J. A. Malikayil, I. M. Armitage, *J. Magn. Reson.* **1988**, *76*, 352–357.
- [30] We used the algorithm published in: W. H. Press, B. P. Flannery, S. A. Teukolsky, W. T. Vetterling *Numerical Recipes in C*, Cambridge University Press, Cambridge (UK), **1989**.
- [31] The chemical shift of the solvent was measured at several different temperatures and was calibrated relative to TMS in [D₈]THF in different concentrations, compare: M. Nir, I. O. Shapiro, R. E. Hoffmann, M. Rabinovitz, *J. Chem. Soc. Perkin Trans. 2* **1996**, 1607–1616.

Received: September 6, 2002 [F4401]